Kobe University Repository : Kernel

PDF issue: 2026-11-12

Effects of rainfall rate on physical characteristics of outdoor noise from the viewpoint of outdoor acoustic mass notification system

Sato, Hayato
Kurisu, Kiyohiro
Morimoto, Masayuki
Maeda, Mitsuki

(Citation)
Applied Acoustics,172:107616

(Issue Date)
2021-01-15

(Resource Type)
journal article

(Version)
Accepted Manuscript

(Rights)
© 2020 Elsevier Ltd. All rights reserved.
This manuscript version is made available under the CC-BY-NC-ND 4.0 license
http://creativecommons.org/licenses/by-nc-nd/4.0/

(URL)
https://hdl.handle.net/20.500.14094/90009294

KOBE UNIVERSITY

Effects of rainfall rate on physical characteristics of outdoor noise from the viewpoint of outdoor acoustic mass notification system

Hayato Sato[a,*], Kiyohiro Kurisu[b], Masayuki Morimoto[a], Mitsuki Maeda[a]

[a]*Environmental Acoustics Laboratory, Department of Architecture, Graduate School of Engineering, Kobe University, Rokko, Nada, Kobe 657-8501, Japan*
[b]*TOA Corporation, Minatojima-Nakamachi, Chuo-ku, Kobe 650-0046, Japan*

Abstract

In Japan, there are many natural disasters that often expose residents to the risk of serious damage. To minimize such damage, the Japanese government has built a disaster information network using a radio system, and as part of it, an outdoor acoustic mass notification system is routinely operated. However, its intelligibility may be reduced by outdoor noise, which is increased by rainfall. In the present study, long-term surveys of rainfall rate and outdoor noise were conducted at four sites with different surrounding environments and the relationship between them was analyzed to clarify the effects of the rainfall rate on the physical characteristics of outdoor noise. The results indicated that the median sound pressure level for each 1/3 octave band increased with increasing rainfall rate, mainly above mid-frequencies of around 500 Hz to 1 kHz, though the frequency at which the level began to rise depended on the time period and site. Furthermore, a newly proposed macroscopic model for estimating the sound pressure level of outdoor

*Corresponding author. Tel./fax: +81 78 803 6052.
Email address: hayato@kobe-u.ac.jp (Hayato Sato)

noise under rainy conditions indicated that the distance from the loudspeaker of the system to ensure a certain speech-to-noise ratio could be significantly reduced by heavy rainfall.
Keywords: Outdoor noise, Mass notification system, Raindrop collision, Speech intelligibility

1. Introduction

In Japan, there are many natural disasters such as earthquakes, typhoons, heavy rain, and tsunamis, which expose residents to the risk of serious damage. To minimize such damage, it is necessary to quickly and accurately transmit disaster information to residents. The Japanese government has built a disaster information network at the national, prefectural, and local levels that uses a radio system, and as part of it, sound information is routinely transmitted over a wide area using an outdoor acoustic mass notification system. In general, a system is adopted in which a slave station consisting of a radio receiver and loudspeakers is installed on a building roof or a dedicated pole and the sound information transmitted from a master station is radiated from the loudspeakers with a high sound pressure level (SPL).

It is well known that outdoor sound propagation is affected by weather conditions. For example, the effects of the vertical distribution of wind speed and temperature on long-distance sound propagation have been studied in detail. When considering sound information transmission, it is necessary to estimate the signal-to-noise ratio, which determines intelligibility. This means that not only the SPL of the sound carrying information transmitted from far away to a listening point but also the SPL of background noise at the point should be estimated. In

other words, the effects of weather on background noise should be investigated.

In recent years, in Japan, damage caused by sudden and localized heavy rain that is difficult to predict has increased. In such cases, it is necessary to transmit evacuation information. The transmission of evacuation information using an outdoor acoustic mass notification system can be effective because an immediate response to such an unexpected situation is possible. However, during rainfall, the SPL and frequency characteristics of outdoor noise change owing to the sound of raindrops colliding with surfaces, and the intelligibility of evacuation information will decrease.

There have been several studies on noise generated by the collision of raindrops, for example, vegetation noise[1] and roof noise[2–6]. Furthermore, changes in traffic noise when a road surface is wet have also been studied[7–10]. Outdoor noise during rainfall is a combination of these factors, and therefore the effects of rainfall will depend on the environment around the measurement point. However, no study could be found on how rainfall changes the physical characteristics of such complex outdoor noise.

The purpose of the present study is to clarify the effects of the rainfall rate, which is the main parameter of rainfall, on the physical characteristics of outdoor noise. As a case study, a long-term survey of rainfall and outdoor noise was conducted at four sites with different surrounding environments. On the basis of the results, the change in outdoor noise due to rainfall and how the change affects the speech intelligibility of information transmitted by an outdoor acoustic mass notification system were analyzed.

2. Methods

Measurements were performed at four sites in Hyogo Prefecture, Japan. The measurement sites were selected to satisfy the following conditions:

(1) Permission to use a building or a lot including a stable electrical power supply was obtained from the owner.

(2) Measurement equipment could be physically isolated from pedestrians.

(3) The characteristics of surfaces on which raindrops impact were different at each site.

Table 1 shows a summary of the measurement sites. Figure 1 shows satellite photos of the measurement sites obtained from Google Earth. The red circles in the photos indicate the measurement points.

[Table 1 about here.]

[Figure 1 about here.]

The measurement equipment consisted of a weather measuring device and a noise measuring device. Both were connected to a tablet PC (Microsoft, Surface 3), and measurement data were uploaded continuously to cloud storage (Dropbox) via the PC. The weather measuring device (Davis, VantagePro2) recorded the temperature, relative humidity, wind speed, and rainfall rate every minute. The noise measurement was performed using a sound level meter (Rion, NL-21) with an all-weather windscreen (Rion, WS-03). The AC output of the sound level meter was transmitted to the PC using an audio unit (Roland, UA-11Mk2). L_{Aeq} and L_{eq} in each 1/3 octave band were calculated from the AC output every minute using

the first 30 s of the sample. Time stamps were also added to both weather and noise data. Therefore, a synchronized set of weather and noise data was obtained every minute. Figure 2 shows the equipment installed at site 2 as an example.

[Figure 2 about here.]

The equipment was operated continuously from early October to the end of November in 2015, though the measurement period varied somewhat among the sites. Note that missing observations occurred intermittently at every site because of the unexpected shutdowns of the PC or the forced terminations of the software used to calculate sound levels. Table 2 shows the measurement periods and the numbers of samples of weather and noise data successfully recorded.

[Table 2 about here.]

3. Results and discussion

3.1. Rainfall rate

Figure 3 shows temporal sequences of the rainfall rate every minute for each site. The unit of rainfall rate is mm/h, and the rainfall rate was estimated from one-minute measurements. Periods colored in grey represent missing observations. Roughly, rainfall was simultaneously observed at all of the sites, because the distance among the sites was 16 km at most. Note that rainfall rates of more than 40 mm/h, which is a typical threshold for a heavy rainfall warning in Japan and is classified as *Heavy* in ISO 10140-5:2010[11], were observed several times in the measurement periods, though such heavy rainfall lasted for a short time.

[Figure 3 about here.]

Table 2 also shows the numbers of samples with rainfall and with a rainfall rate of more than 40 mm/h for each site. In the following sections, the samples are classified into two groups: *without rainfall* for the samples with zero rainfall rate, and *with rainfall* for the samples with nonzero rainfall rate.

3.2. Outdoor noise without rainfall

The physical characteristics of outdoor noise for *without rainfall* are required as a reference to analyze the effects of rainfall on outdoor noise. In this section, factors of outdoor noise for *without rainfall* at the sites are investigated to classify the measured samples. The main noise sources at the sites were traffic noise, aircraft noise, and sound from pedestrians. In many cases, the frequency characteristics of these sources are broadband spectra rather than line spectra. Therefore, L_{Aeq} for each sample was first analyzed as a representative measure.

3.2.1. Effect of measurement time

Figure 4 shows the time sequence of L_{Aeq} from 2nd (Mon.) to 8th (Sun.) November 2015 for each site as an example. Discontinuous periods were missing observations or *with rainfall*. Daily cycles of L_{Aeq} were clearly found and the time pattern for each cycle was similar for all days of the week at each site.

[Figure 4 about here.]

However, the dynamic ranges of L_{Aeq} variation in each daily cycle were different at different sites. The dynamic ranges for sites 1 and 2 were around 20 dB (site 1: 40–60 dB, site 2: 50–70 dB), excluding some sporadic high L_{Aeq} values. The range for site 4 was around 35 dB (40–75 dB), which was the widest

among the sites. Sites 2 and 4 had similar features, as shown in Table 1, and the main noise source at these sites was road traffic noise. The decrease in the lower limit of the range of site 4 relative to site 2 might have been related to the fact that the traffic of the road beside site 2 is heavier than that beside site 4. The microphone of site 4 was installed at a lower position than that of site 2, and the distance between the microphone and the road can explain the increase in the upper limit of site 4 relative to site 2.

The daily cyclic pattern for site 3 was different from those for the other sites at first glance. Samples with L_{Aeq} of 60 to 65 dB were frequently observed from 07:00 to 21:00. An airport is located near sites 2, 3, and 4, and the normal take-off flight path of the airport was close to site 3. Because of the location of site 3 and the flight schedule of the airport, it is likely that the L_{Aeq} for this site values were strongly affected by aircraft noise.

Therefore, the samples with a strong effect of aircraft noise were extracted with reference to the L_{eq} of the low-frequency band, which is hardly affected by rainfall, and they were excluded from the analysis. In particular, the samples with L_{eq} of more than 60 dB in the 63 Hz band were excluded for site 3 only.

Figure 5 shows the median and 90% range of L_{Aeq} for the *without rainfall*. The statistics were calculated hourly for each site. The median of L_{Aeq} started to rise after 04:00, and remained high between 07:00 and 17:00, and then decreased gradually. This tendency was common to all of the sites. Although the width of the 90% range had different dynamic ranges at different sites, its time sequence showed the same trend as the median of L_{Aeq}. The differences between the maximum and minimum values of the median of L_{Aeq} were 8.4, 11.2, 7.4, and 20.9 dB for sites 1 to 4, respectively.

[Figure 5 about here.]

It can be assumed that the effect of rainfall on outdoor noise depends on the ratio of the energy of outdoor noise under no rainfall conditions to that of sounds caused by rainfall. Therefore, the wide dynamic ranges of the median of L_{Aeq} indicate that the outdoor noise obtained here should be classified by the time of day of the measurement. Hereafter, data are analyzed in two periods of time, 01:00–04:59 (*NT*) and 07:00–17:59 (*DT*), because the statistics of L_{Aeq} in these periods were temporally flat relative to those in other periods of time as shown in Fig. 5.

3.2.2. Effects of other weather parameters

As described in section 2, temperature, relative humidity, and wind speed were measured as weather parameters other than rainfall rate. The relationships between L_{Aeq} and the parameters for *without rainfall* samples were analyzed. It was found that L_{Aeq} was not systematically affected by temperature and relative humidity; however, L_{Aeq} increased with increasing wind speed. The main sources of the wind noise are thought to be the rustling of leaves[1] (sites 1 and 2) and air turbulence[12, 13] (all sites).

The weather measuring device used in the present study records wind speed in steps of 1 mi/h. In the present study, the unit of the wind speed was converted from mi/h to m/s as follows: (1) multiplied by 1609 to convert miles to meters, (2) divided by 3600 to covert hours to seconds, and (3) rounded to the first decimal place. Figure 6 shows the median of L_{Aeq} as a function of wind speed, and the cumulative frequency of wind speed for each site and time period. The wind noise measured by Lin *et al.*[13] with the same wind screen (Rion, WS-03) is

also shown in Fig. 6. Lin *et al*. demonstrated that the wind speed in the wind screen was 0.0 m/s and that the maximum increase in L_{Aeq} was 0.7 dB unless the outside wind speed exceeded 2.0 m/s. In the data measured in the present study, the maximum median of L_{Aeq} relative to that at zero wind speed was also around 1 dB regardless of the site and time period unless the wind speed exceeded 2.0 m/s. The median of L_{Aeq} began to increase in some cases when the wind speed exceeded 2.0 m/s. However, the cumulative frequency of the wind speed showed that the samples with a wind speed less than 2.0 m/s accounted for more than 90% of the samples in many cases. Although the samples with a wind speed more than 2.0 m/s were more frequently found at sites 2 and 3 in *DT* than in other cases, the slopes of L_{Aeq} with respect to the wind speed in the two cases were shallow.

From the above, it is considered that the effects of temperature, relative humidity, and wind speed were negligible as a whole, and the classification of samples based on these parameters was not carried out in the following analyses.

[Figure 6 about here.]

3.2.3. Frequency characteristics of L_{eq} without rainfall

The frequency characteristic of *without rainfall* for the two time periods (*NT* and *DT*) was obtained as a reference for analyzing the effect of rainfall. Figure 7 shows the median and 90% range of L_{eq} for each 1/3 octave band.

[Figure 7 about here.]

At all sites, the statistics of L_{eq} for *DT* was higher than that for *NT*, but there was no significant difference in frequency characteristic between *NT* and *DT*.

The frequency characteristics can be roughly divided into two types. For sites 1 and 3, over a wide frequency range, the median of L_{eq} decreased about 3 to

4 dB with a doubling of the center frequency of 1/3 octave band. This slope was similar to that for the type of noise referred to as 'red noise' which has amplitude inversely proportional to the frequency. For sites 2 and 4, the median of L_{eq} was almost flat at 1.25 kHz or less and decreased with increasing frequency in the higher range. As shown in Table 1, sites 2 and 4 were beside a main road, and their frequency characteristics agreed with that of road traffic noise[14]. From the above, it can be considered that the frequency characteristics of sites 2 and 4 were almost completely determined by road traffic noise from the nearby major road. For sites 2 and 4, the absolute values of the median of L_{eq} were almost identical between the sites for DT, but the absolute values of the median of L_{eq} for site 4 were lower than those of site 2 for NT. It is reasonable to conclude that this was due to the difference in road traffic in NT. Because at the upper limit of the 90% range, this can be regarded as the result when the traffic was heavy, there was no significant difference between the two sites for NT.

The median and the lower limit of the 90% range for site 1 in DT might have an intermediate characteristic between the road traffic noise type and the red noise type. It is considered that they were affected by distant traffic noise when the surroundings were quiet, as the altitude of site 1 was about 120 m and the distant city could be seen.

3.3. Outdoor noise with rainfall

The sound power of rain noise from a roof surface increases with increasing rainfall rate as the number of collisions per unit time increases. For artificial rain, the noise level increases by about 10 dB per 10-fold increase in rainfall rate[5]. For natural rain, the noise level increases by 10 dB or more per 10-fold increase in rainfall rate because the radius and terminal velocity of of raindrops increase

with the rainfall rate. Specifically, the increase is about 15 to 20 dB[2, 3].

The sounds caused by rainfall are not only the rain noise on roofs. However, the relationship between their total SPL and the rainfall rate is expected to be a logarithmic function similarly to the case of rain noise on roofs. Considering not only the logarithmic relationship but also the balance of the number of samples included in each classification, the rainfall rate was divided into the five classes shown in Table 3. The numbers of *with rainfall* for each classification, site, and time period are also shown in Table 3. For site 3, the samples with L_{eq} of more than 60 dB at 63 Hz band were excluded as in the case of *without rainfall*.

[Table 3 about here.]

Table 4 shows the medians of rainfall rate, temperature, and relative humidity, and the average wind speed for each classification of rainfall rate. For the wind speed, the average was used as a representative value because of the lower measurement resolution. The average wind speed was less than 2.0 m/s under almost all conditions; thus, the effect of the wind speed on the results was negligible.

[Table 4 about here.]

3.3.1. Relationship between rainfall rate and L_{Aeq}

For each classification in Table 3, statistics of the rainfall rate and L_{Aeq} were calculated. Figure 8 shows the relationship between them in scattergrams. The rainfall rate on the horizontal axis has a logarithmic scale. For reference, the statistics of L_{Aeq} for *without rainfall* are also shown in Fig. 8.

[Figure 8 about here.]

For many combinations of time period and site, the statistics of L_{Aeq} tended to increase linearly with the logarithmic rainfall rate. There were differences in slope among the combinations. The slope became steeper as L_{Aeq} for *without rainfall* decreased. For example, at site 1, the median of L_{Aeq} was 44.3 dB and the difference between the maximum and the minimum rainfall rates was 10.5 dB for *NT*, while the median of L_{Aeq} was 51.5 dB and the difference was 5.1 dB for *DT*.

In order to analyze the SPL of the sounds caused by rainfall, $L_{\mathrm{CRF}}(RR)$ defined by Eq. 1 was obtained as

$$L_{\mathrm{CRF}}(RR) = 10\log_{10}\left(10^{L_{\mathrm{Aeq}}(RR)/10} - 10^{L_{\mathrm{Aeq}}(0)/10}\right), \tag{1}$$

where $L_{\mathrm{Aeq}}(0)$ is the median of L_{Aeq} without rainfall and $L_{\mathrm{Aeq}}(RR)$ is the median of L_{Aeq} when the median of the rainfall rate is RR. Figure 9 shows scattergrams of $L_{\mathrm{CRF}}(RR)$ and the median of the rainfall rate for each classification shown in Table 3. Trends were divided into two groups, sites 1 and 3 and sites 2 and 4, from the viewpoint of differences due to the time period.

[Figure 9 about here.]

Sites 1 and 3

In the group of sites 1 and 3, the absolute value of $L_{\mathrm{CRF}}(RR)$ was not strongly affected by the time period. However, the slope of $L_{\mathrm{CRF}}(RR)$ plotted against rainfall rate was steeper for *NT* than for *DT*. The slopes were similar to that for the rain noise on roofs, which is 10 dB or more per 10-fold increase in rainfall rate, except for *DT* at site 1. This indicates that the sounds caused by rainfall at the sites primarily consisted of those caused by the collision of raindrops with other objects.

For both time periods, the slopes were steeper for site 3 than for site 1. One reason why the slopes differed between sites 1 and 3 might have been the effect of traffic noise in site 1 as mentioned in 3.2.3. As an alternative reason, it is possible to consider the difference in the type of object with which raindrops collide. The main object was leaves of surrounding trees for site 1, whereas it was gravel on the ground for site 3. These objects differed in shape and mass, and it is clear from the theory suggested by Griffin and Ballagh[5] that the sounds caused by the collision of raindrops depend on such parameters.

$L_{\mathrm{CRF}}(RR)$ for site 1 was 10–15 dB higher than that for site 3. If the above alternative reason was valid, then the leaves of the surrounding trees would generate louder sounds by raindrop collision than gravel on the ground.

Sites 2 and 4

In the group of sites 2 and 4, both the absolute value and the slope were clearly affected by the time period. For *NT*, $L_{\mathrm{CRF}}(RR)$ increased by about 9–10 dB per 10-fold increase rainfall rate. The slopes for *DT* were shallower than those for *NT*, and the slopes were 3–4 dB per 10-fold increase in rainfall rate.

As described in 3.2.3, traffic noise was dominant for *DT* at sites 2 and 4. Ishikawa *et al.*[8] reported that the L_{Aeq} of noise from moving vehicles increased by 2–5 dB under light rain conditions (average rainfall rate = 3 mm/h) compared with that on sunny days, depending on the type of pavement (dense-graded or drainage). The noise from moving vehicles on rainy days depends on puddles on the road surface, and its relationship with the rainfall rate is not expected to be explained by the same theory as that for the rain noise on roofs. Considering the shallow slopes of $L_{\mathrm{CRF}}(RR)$ for *DT*, the effect of the rainfall rate on the L_{Aeq} of noise from moving vehicles should be small. Note that the pavements of the roads

adjacent to sites 2 and 4 were of the drainage type, suppressing the increase in noise from moving vehicles due to rainfall[8].

For *NT*, the raindrop collision sound could have been more dominant than the noise from moving vehicles because of the decrease in traffic volume, and as a result, the slopes of $L_{\mathrm{CRF}}(RR)$ might have approached those for the rain noise on roofs. The difference in $L_{\mathrm{CRF}}(RR)$ between *NT* and *DT* was around 15 dB for the lowest rainfall rate, but it decreased with increasing rainfall rate. This indicates that the raindrop collision sound in unusually heavy rain, such as a rainfall rate of more than 100 mm/h, will exceed the noise from moving vehicles even for *DT*, and the slopes for *DT* will become steeper under such conditions.

The higher $L_{\mathrm{CRF}}(RR)$ for site 4 than for site 2 might be due to differences in the surrounding buildings. There were large concrete buildings and many open spaces around site 2, while there were wooden houses with a high density around site 4 (see Fig. 1).

3.3.2. Relationship between rainfall rate and frequency characteristic of L_{eq}

To avoid redundancy by discussing all the statistical values, only the frequency characteristic of the median of L_{eq} is analyzed as a representative characteristic here. Figure 10 shows the median of L_{eq} for each 1/3 octave band and classification shown in Table 3. Different symbols represent different rainfall rate classifications. Dashed lines are the results for *without rainfall* shown in Fig. 7.

[Figure 10 about here.]

The median of L_{eq} increased with increasing rainfall rate mainly above mid-frequencies of around 500 Hz to 1 kHz, though the frequency at which it began to increase depended on the time period and site. From this result, it is

considered that the sounds caused by rainfall had stronger frequency components than the outdoor noise for *without rainfall* above the mid-frequencies, in the range of the rainfall rate observed in the present study. The effect of the rainfall rate on L_{eq} above mid-frequencies was smaller for *DT* than for *NT*, which was particularly clear for sites 2 and 4. This tendency was consistent with the slopes of $L_{\mathrm{CRF}}(RR)$ shown in Fig. 9.

To compare the frequency characteristics of the sounds caused by rainfall at the same rainfall rate, the band level of the sound for a certain rainfall rate was estimated. Firstly, $L_{\mathrm{CRF}}(RR, i)$, which is the band level of the sounds caused by rainfall with a rainfall rate of RR for band i, was calculated as

$$L_{\mathrm{CRF}}(RR, i) = 10 \log_{10} \left(10^{L_{\mathrm{eq}}(RR,i)/10} - 10^{L_{\mathrm{eq}}(0,i)/10} \right), \tag{2}$$

where $L_{\mathrm{eq}}(0, i)$ is the median of L_{eq} without rainfall for band i and $L_{\mathrm{eq}}(RR, i)$ is the median of L_{eq} for band i where the median of the rainfall rate is RR. Then, $\hat{L}_{\mathrm{CRF}}(RR, i)$ for a certain RR was estimated by linear regression analysis between $L_{\mathrm{CRF}}(RR, i)$ and the median rainfall rate for each band. The estimated level was adopted when the correlation coefficient for the regression analysis was statistically different from zero ($p = 0.05$), in other words, when the correlation coefficient was larger than 0.997, 0.950, and 0.878 for 3, 4, and 5 samples, respectively.

Figure 11 shows $\hat{L}_{\mathrm{CRF}}(RR, i)$ for RR values of 3 and 30 mm/h. These two RR values were respectively chosen to represent light and heavy rain conditions within the range of interpolation or slight extrapolation of the regression equations. Considering the results of $L_{\mathrm{CRF}}(RR)$ shown in Fig. 9, the results of $\hat{L}_{\mathrm{CRF}}(RR, i)$ are divided into the two groups of sites and analyzed.

[Figure 11 about here.]

Sites 1 and 3

For both sites 1 and 3, $\hat{L}_{\mathrm{CRF}}(RR, i)$ in *DT* was slightly higher than that in *NT* for *RR* of 3 mm/h, but the differences almost disappeared for *RR* of 30 mm/h. This tendency was expected from the regression lines shown in Fig. 9. The frequency characteristics for *RR* of 30 mm/h can be regarded as those for the sound caused by raindrop collisions because $\hat{L}_{\mathrm{CRF}}(RR, i)$ in *DT* was almost the same as that in *DT*. The characteristics were similar for sites 1 and 3. The characteristics were almost flat within the range of 1–4 kHz and decayed at higher frequencies. However, the absolute values for site 1 were 5–10 dB higher than those for site 3, and it is highly probable that this was caused by the difference in the type of object against which raindrops collided, as mentioned in 3.3.1.

Sites 2 and 4

In many cases, $\hat{L}_{\mathrm{CRF}}(RR, i)$ could not be obtained at medium or low frequencies because the median of L_{eq} did not depend on the rainfall rate at these frequencies. For *RR* of 3 mm/h, at frequencies above 1 kHz, the frequency characteristics showed steep slopes and $\hat{L}_{\mathrm{CRF}}(RR, i)$ decreased about 6 to 8 dB with a doubling of the center frequency of 1/3 octave band. $\hat{L}_{\mathrm{CRF}}(RR, i)$ in *DT* was clearly higher than that in *NT*, though the difference was smaller for site 4 owing to the shallow slope in *NT* relative that for site 2. For *RR* of 30 mm/h, there were differences between sites 2 and 4. For site 2, the characteristics retained their steep slopes and the clear difference in $\hat{L}_{\mathrm{CRF}}(RR, i)$ for different time periods. For site 4, the slopes became shallower than those for *RR* of 3 mm/h in both time periods, and $\hat{L}_{\mathrm{CRF}}(RR, i)$ in *NT* approached that in *DT*. The negligible difference in $\hat{L}_{\mathrm{CRF}}(RR, i)$ between *NT* and

DT with different traffic volumes suggests that the raindrop collision sound was more dominant than the traffic noise.

From the above results, it can be concluded that the steep slope was due to noise from moving vehicles on a wet road, whereas the shallow slope observed at site 4 was the result of an increase in the energy of the raindrop collision sound relative to that of traffic noise. This is consistent with the inference in 3.3.1 that the effect of the raindrop collision sound was stronger at site 4 than at site 2 because of the high density of surrounding buildings.

4. General discussion

4.1. Macroscopic model of outdoor noise under rainy condition

The measurement results demonstrated that the rainfall rate affected the traffic noise and raindrop collision sound differently, and that the SPL of the raindrop collision sound depended on the surface material in the surrounding environment. In addition, the effect of the rainfall rate became strong as the SPL for *without rainfall* decreased. From these results, it is worth considering the following macroscopic model to estimate the SPL of outdoor noise under rainy conditions:

$$L(RR) = 10 \log_{10} \sum_{k=1}^{n} E_k RR^{a_k}, \tag{3}$$

where $L(RR)$ is the SPL of outdoor noise when the rainfall rate is RR, E_k is the sound energy for element k, which constitutes outdoor noise at a rainfall rate of 1 mm/h, and a_k is a parameter that determines the effect of the rainfall rate on element k.

a_k is a real number greater than or equal to zero (assuming that $0^0 = 1$). As a_k approaches zero, the sound energy of the element approaches a constant value

regardless of the rainfall rate, and as a_k becomes larger, the sound energy of the element more rapidly increases with increasing rainfall rate. When outdoor noise consists of a single element ($n = 1$), the SPL of the outdoor noise increases by $10a_1$ dB per 10-fold increase in rainfall rate.

If element k represents traffic noise, E_k will be determined by the traffic volume and the type of pavement, while a_k will only be determined by the type of pavement. If element k represents the raindrop collision sound, E_k will be determined by the physical properties of the collision surface, while a_k will be determined by the number of collisions per unit time and the size of raindrops.

We attempted to estimate the median of L_{Aeq} from this model. The elements constituting outdoor noise were classified into sound existing regardless of the presence or absence of rainfall and sound resulting from rainfall, and the latter was further divided into two sounds derived from the change in the road surface condition (dry/wet/with puddles) and raindrop collisions.

The sound existing regardless of the presence or absence of rainfall was estimated from the results of *without rainfall* shown in Fig. 8 (horizontal solid line). a_k is zero for this sound.

The sound derived from raindrop collisions was estimated from the results of Fig. 9 in NT as the closest value. E_k was the constant term of the regression equation in Fig. 9, that is, the estimated value of $L_{\mathrm{CRF,1mm/h}}$. a_k was obtained by dividing the slope of the regression equation by 10.

For the sound derived from the change in the road surface condition, estimations of E_k and a_k were difficult. Here, E_k in NT was set to zero, and that in DT was obtained from the energy difference between the constant terms of the regression equations for DT and NT. The values of a_k for sites 2 and 4

were obtained by dividing the slope of the regression equation for DT, that is, the measurement time during which traffic noise was dominant, by 10. The values of a_k for sites 1 and 3 were set at 0.3, which is the average of the values for sites 2 and 4, because the effect of traffic noise was unknown. For example, Eq. 4 describes the model of $L(\mathrm{RR})$ for site 1 in DT.

$$L(\mathrm{RR}) = 10\log_{10}\left(10^{51.5/10}RR^{0} + 10^{45.4/10}RR^{0.834} + \left(10^{50.1/10} - 10^{45.4/10}\right)RR^{0.3}\right) \quad (4)$$

Figure 12 shows the medians of L_{Aeq} estimated from the macroscopic model for each pair of site and time period. The measured values were equal to those shown in Fig. 8. The determination coefficients between the measured and estimated values ranged from 0.83 to 0.99, and the overall shapes of the measured values and estimated curves coincided for all pairs of site and time period. Therefore, it can be concluded that the macroscopic model was valid within the range of the data obtained in the present study, though there is still much room to optimize the sound classification and estimation methods for each parameter.

[Figure 12 about here.]

4.2. Effect of rainfall on outdoor acoustic mass notification system

In this section, the maximum distances from the loudspeaker to maintain a certain speech-to-noise ratio in heavy rain are estimated to discuss the effect of rainfall on an outdoor acoustic mass notification system. The speech-to-noise ratio here is defined as the difference in L_{Aeq} between the amplified speech provided by the system and the background noise at the listening point.

Table 5 shows the medians of L_{Aeq} estimated from the macroscopic model shown in Fig. 12 for rainfall rates of 0, 40, 80, and 160 mm/h. These values were used as the background noise level regardless of the distance from the loudspeaker to calculate the speech-to-noise ratio.

[Table 5 about here.]

Next, we estimate the speech level at a certain distance from the speaker of the system. First, we quantify the effect of atmospheric absorption on the A-weighted SPL of speech. Atmospheric absorption coefficients in ISO 9613-1:1993[15] for a temperature of 15°C and a relative humidity of 90% were used, considering the measured data shown in Table 4. Although the relative humidity dropped to about 60 to 70% for *without rainfall*, the combination of the above temperature and relative humidity was used for all conditions because there was almost no difference observed in the results. The frequency characteristic of speech was assumed to be that for the vocal effort of *Normal* given in the standard for calculating the speech intelligibility index (SII)[16]. In the calculation example here, the data in 1/3 octave bands from 160 Hz to 8 kHz were used. When a point 1 m from the loudspeaker is the reference point, the attenuation of the A-weighted SPL of speech due to the atmospheric absorption at a point of r m from the loudspeaker ($\Delta L_{\mathrm{A,absb}}(r)$) can be obtained as

$$\Delta L_{\mathrm{A,absb}}(r) = 10\log_{10}\sum_{i=1}^{18} 10^{\frac{L_{i,Normal}(1)-\alpha_i(r-1)+Aw_i}{10}} - L_{\mathrm{A},Normal}(1), \tag{5}$$

where α_i dB/m is the atmospheric absorption coefficient for band i, Aw_i dB is the A-weighting correction value for band i, $L_{i,Normal}(1)$ is the SPL of speech with *Normal* vocal effort for band i at a distance of 1 m from the loudspeaker, and

$L_{A,Normal}(1)$ dB is the A-weighted SPL of speech at a distance of 1 m from the loudspeaker. $L_{A,Normal}(1)$ can be obtained from the energy sum of $L_{i,Normal}(1) + Aw_i$. Using the values given in the standard for SII, $L_{A,Normal}(1)$ is calculated to be 59.2 dB. Figure 13 shows $\Delta L_{\mathrm{A,absb}}(r)$ at distances from 1 to 5000 m obtained using Eq. 5.

[Figure 13 about here.]

The A-weighted SPL of amplified speech at a distance of r m from the loudspeaker ($L_{\mathrm{A}}(r)$) can be obtained from Eq. 6, assuming that the loudspeaker is omnidirectional and that the distance attenuation does not depend on the sound frequency.

$$L_{\mathrm{A}}(r) = L_{\mathrm{A}}(1) + \Delta L_{A,absb}(r) - 20\log_{10} r \tag{6}$$

Here, $L_{\mathrm{A}}(1)$ [dB/m] is the A-weighted SPL of amplified speech. For the loudspeakers used in Japan, the maximum SPL at a distance of 1 m from the loudspeaker is around 125 dB. When the SPL of amplified speech with the frequency characteristic of *Normal* vocal effort is 125 dB, its A-weighted SPL is calculated to be 121.9 dB. Therefore, $L_{\mathrm{A,\ 1m}}$ is set to 121.9 dB.

Table 6 shows the maximum distances from the loudspeaker to maintain a speech-to-noise ratio of more than +6 dB, as examples criteria to ensure a certain degree of intelligibility. For each combination of site, time period, and rainfall rate, values were determined in 1 m steps, using the ratio obtained by subtracting the estimated background noise level shown in Table 5 from $L_{\mathrm{A}}(r)$. Under no rainfall condition, the ratio of +6 dB or more can be achieved, even at a distance on the order of kilometers, except for sites 2 and 4 in *DT* where traffic noise was

dominant. However, under heavy rain conditions such as a rainfall rate of more than 40 mm/h, the maximum distances decreased to the order on 100 m regardless of the site and time period.

These calculations clearly show that it is necessary to devise a means of coping with such a reduction in the coverage of the loudspeaker due to heavy rain. For example, the design of a system with a margin for the maximum sound output by spatially densifying the loudspeaker arrangement or adopting a loudspeaker with less distance attenuation may be possible. Moreover, the introduction of a movable mass notification system, such as a car, an unmanned aerial vehicle, is also worth considering.

[Table 6 about here.]

5. Conclusion

In the present study, long-term surveys of rainfall rate and outdoor noise were conducted at four sites with different surrounding environments and the relationship between them was analyzed to clarify the effects of the rainfall rate on the physical characteristics of outdoor noise. The results are summarized as follows.

(1) L_{Aeq} tended to increase linearly with the logarithm of the rainfall rate; however, the slopes were different at different sites and time periods. The slopes became steep as L_{Aeq} for the no rain condition decreased because the raindrop collision sound became more dominant than other sounds.

(2) The L_{eq} for each 1/3 octave band increased with increasing rainfall rate, mainly above mid-frequencies of around 500 Hz to 1 kHz, though the

frequencies at which the level began to increase depended on the site and time period.

(3) A macroscopic model for estimating the sound pressure level under rainy conditions was proposed, and its validity was confirmed from the high determination coefficients of 0.83 to 0.99 within the range of the data obtained in the present study.

(4) Calculations of the coverage of outdoor acoustic mass notification systems indicated that the distance to ensure a certain speech-to-noise ratio could be significantly reduced by heavy rainfall.

Acknowledgments

The research was partially funded by the Promotion Program for Scientific Fire and Disaster Prevention Technologies of the Fire and Disaster Management Agency of Japan (2015). The authors would like to thank Itami City and Itami City Fire Department for their cooperation in the long-term field measurement.

[1] L. N. Miller, Sound levels of rain and of wind in the trees, Noise Control Eng. J. 11 (1978) 101–115.

[2] P. Dubout, The sound of rain on a steel roof, Journal of Sound and Vibration 10 (1) (1969) 144–150.

[3] K. Ballagh, Noise of simulated rainfall on roofs, Applied Acoustics 31 (1990) 245–264.

[4] J. McLoughlin, D. J. Saunders, R. D. Ford, Noise generated by simulated rainfall on profiled steel roof structures, Applied Acoustics 42 (1994) 239–255.

[5] D. Griffin, K. Ballagh, A consolidated theory for predicting rain noise, Journal of Building Acoustics 19 (4) (2012) 221–248.

[6] Y. Xiang, L. Shuai, L. Junjie, Experimental studies on the rain noise of lightweight roofs: Natural rains vs artificial rains, Applied Acoustics 106 (2016) 63–76.

[7] E. F. Freitas, P. A. A. Pereira, L. G. P. Santos, A. P. S. Santos, Traffic noise changes due to water on porous and dense asphalt surfaces, Road Materials and Pavement Design 10 (3) (2009) 587–607.

[8] K. Ishikawa, R. Fukui, H. Nagaoka, E. Noguchi, J. Inoue, A study on the acoustical property of drainage porous asphalt pavement in rain, Proc. of the Meeting the Institute of Noise Control Engineering of Japan (2010) 140–142 (in Japanese).

[9] J. Alonso, J. M. López, I. Pavón, M. Recuero, C. Asensio, G. Arcas, A. Bravo, On-board wet road surface identification using tyre/road noise and Support Vector Machines, Applied Acoustics 76 (2014) 407–415.

[10] M. Cai, S. Zhong, H. Wang, Y. Chen, W. Zeng, Study of the traffic noise source intensity emission model and the frequency characteristics for a wet asphalt road, Applied Acoustics 123 (2017) 55–63.

[11] ISO 10140-5:2010 Am1:2014 Acoustics – Laboratory measurement of

sound insulation of building elements – Part 5: Requirements for test facilities and equipment AMENDMENT 1: Rainfall sound, 2014.

[12] G. F. Hessler, D. M. Hessler, P. Brandstättc, K. Bay, Experimental study to determine wind-induced noise and windscreen attenuation effects on microphone response for environmental wind turbine and other applications, Noise Control Eng. J. 56 (4) (2008) 300–309.

[13] I.-C. Lin, Y.-R. Hsieh, P.-F. Shieh, H.-C. Chuang, H.-C., L.-C. Chou, The effect of wind on low frequency noise, Proc. of Inter Noise 2014 (2014) 1–12.

[14] The Research Committee on Road Traffic Noise in the Acoustical Society of Japan, ASJ Prediction Model 2008 for road traffic noise: Report from the Research Committee on Road Traffic Noise in the Acoustical Society of Japan, J. Acoust. Jpn. 65 (4) (2009) 179–232 (in Japanese).

[15] ISO 9613-1:1993 Acoustics – Attenuation of sound during propagation outdoors – Part 1: Calculation of the absorption of sound by the atmosphere, 1993.

[16] ANSI S3.5-1997, American National Standard Methods for the Calculation of the Speech Intelligibility Index, 1997.

List of Figures

1 Satellite photos of the measurement sites obtained from Google Earth. The measurements were performed at the red circle in each photo. 28
2 Example of installed equipment (Site 2). 29
3 Temporal sequence of rainfall rate for each site. Periods colored in grey represent missing observations. 30
4 Time sequences of L_{Aeq} for the week from 2nd to 8th Nov. 2015. Samples of *with rainfall* were omitted. 31
5 Time sequence of statistics of L_{Aeq} without rainfall for each site. Solid and dashed lines represent the median and 90% range, respectively. 32
6 Effect of wind speed on L_{Aeq} without rainfall for each site and time period. The upper panel shows the median of L_{Aeq} as a function of wind speed, and the lower panel shows the cumulative frequency of wind speed. 33
7 1/3 Octave band spectrum of statistics of L_{eq} without rainfall for each site and time period. Solid and dashed lines represent the median and 90% range, respectively. 34
8 Relationship between rainfall rate and L_{Aeq}. Solid and dashed lines represent the median and 90% range of L_{Aeq} for *without rainfall* respectively. Circles and error bars represent the median and 90% range of L_{Aeq} and rainfall rate for *with rainfall*, respectively. 35
9 Relationship between rainfall rate and L_{Aeq} of the sounds caused by rainfall ($L_{\mathrm{CRF}}(RR)$). Solid and dashed lines represent regression lines for each condition. Different symbols represent different pairs of site and time period. 36
10 1/3 Octave band spectrum of the median of L_{eq} with rainfall for each site and time period. Dashed lines represent L_{eq} for *without rainfall* as a reference. Different symbols represent different rainfall rate (*RR*) classifications. 37
11 Estimated L_{eq} of the sounds caused by rainfall for each 1/3 octave band. Left and right panels show results for rainfall rates (*RR*s) of 3 and 30 mm/h, respectively. Different symbols represent different pairs of site and time period. 38

12 Measured and estimated medians of L_{Aeq} for each pair of site and time period. The estimated values were obtained from the macroscopic model defined by Eq. 3. 39
13 Attenuation of A-weighted level of speech by atmospheric absorption as a function of distance from loudspeaker ($\Delta L_{\mathrm{A,absb}}$), where temperature is 15°C and relative humidity is 90%. 40

Figure 1: Satellite photos of the measurement sites obtained from Google Earth. The measurements were performed at the red circle in each photo.

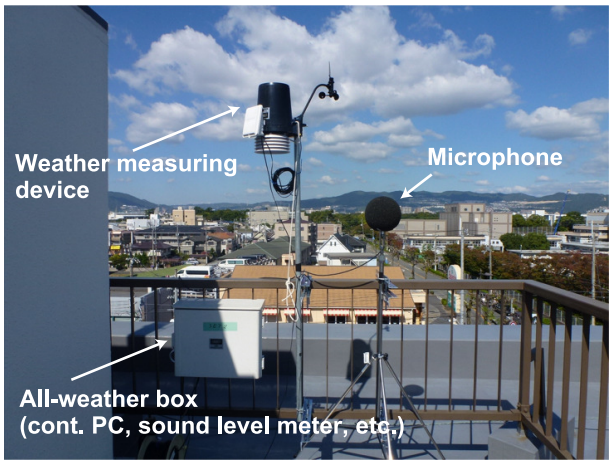

Figure 2: Example of installed equipment (Site 2).

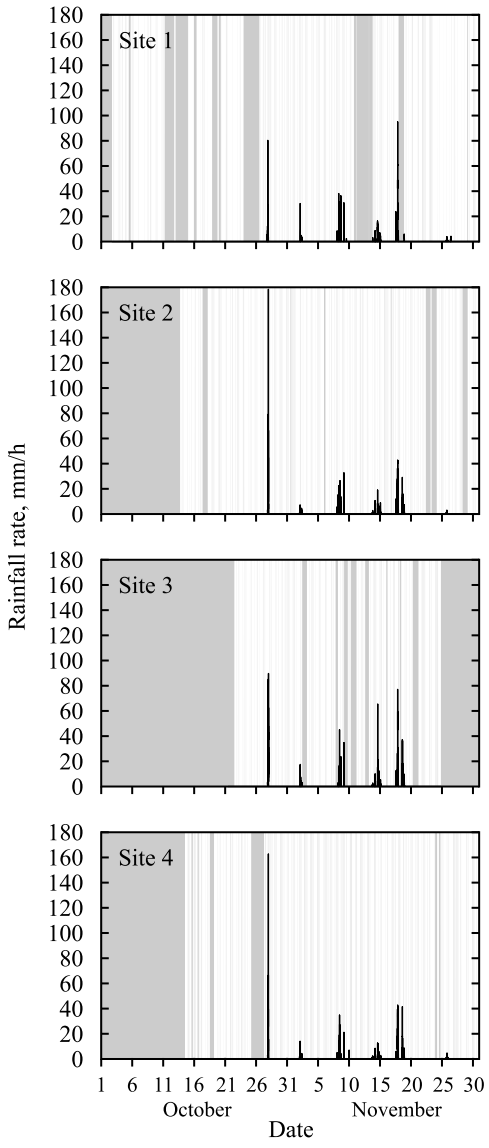

Figure 3: Temporal sequence of rainfall rate for each site. Periods colored in grey represent missing observations.

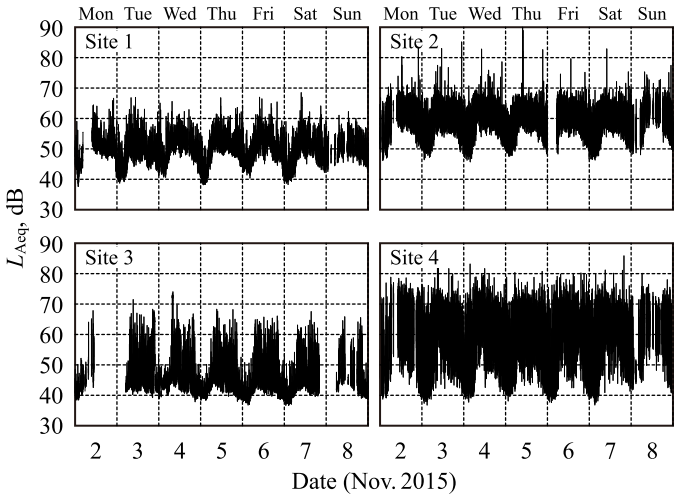

Figure 4: Time sequences of L_{Aeq} for the week from 2nd to 8th Nov. 2015. Samples of *with rainfall* were omitted.

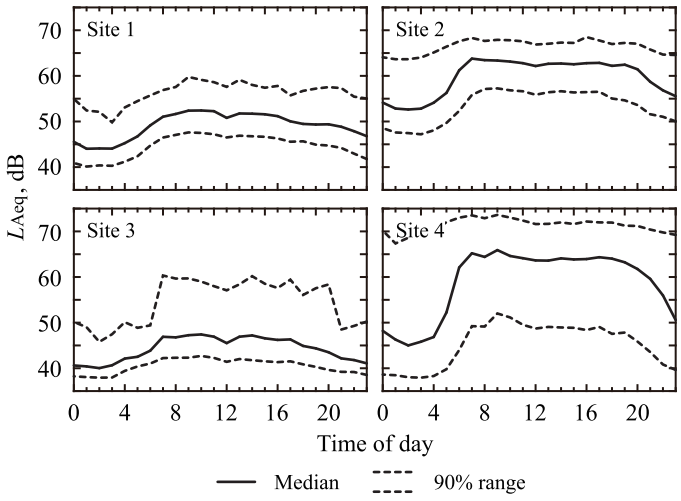

Figure 5: Time sequence of statistics of L_{Aeq} without rainfall for each site. Solid and dashed lines represent the median and 90% range, respectively.

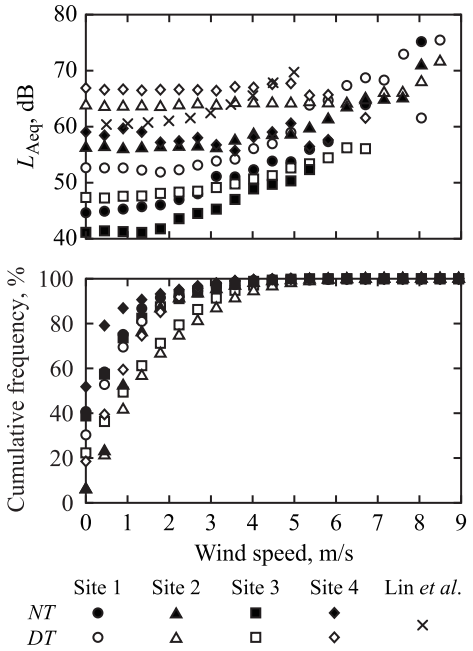

Figure 6: Effect of wind speed on L_{Aeq} without rainfall for each site and time period. The upper panel shows the median of L_{Aeq} as a function of wind speed, and the lower panel shows the cumulative frequency of wind speed.

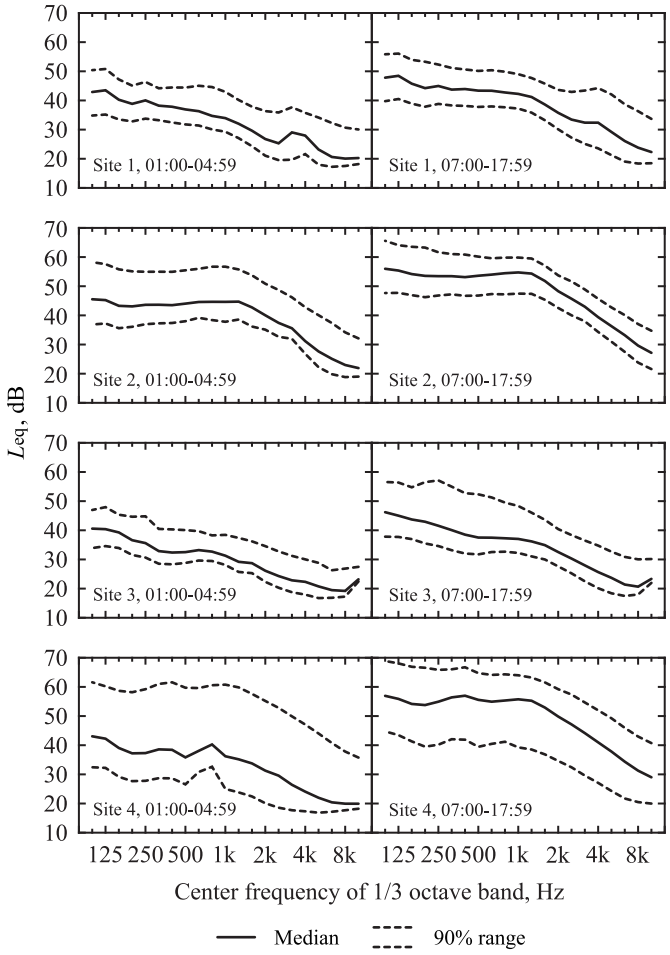

Figure 7: 1/3 Octave band spectrum of statistics of L_{eq} without rainfall for each site and time period. Solid and dashed lines represent the median and 90% range, respectively.

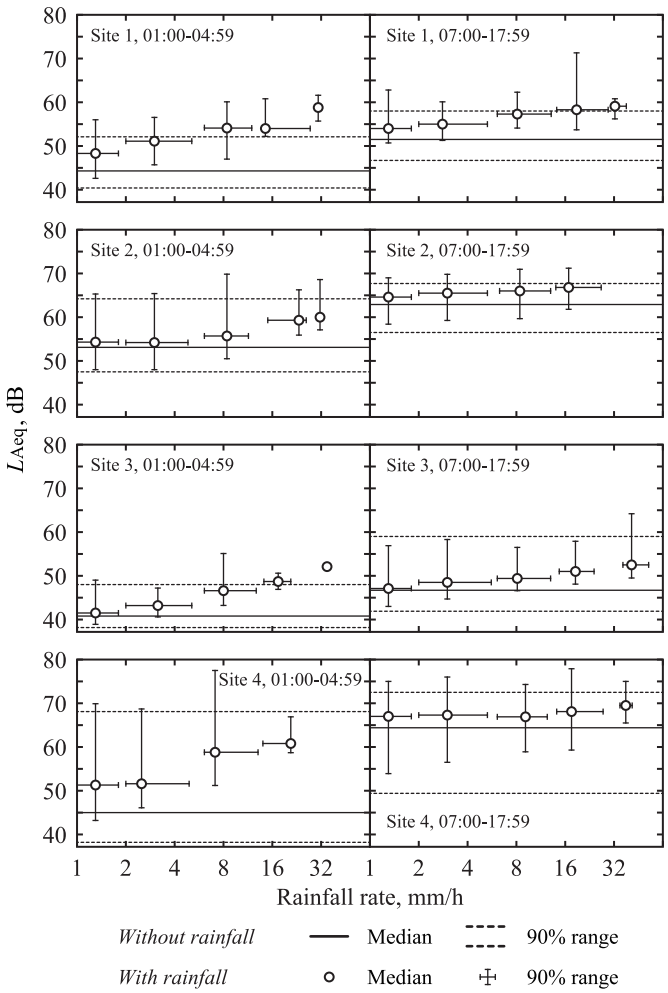

Figure 8: Relationship between rainfall rate and L_{Aeq}. Solid and dashed lines represent the median and 90% range of L_{Aeq} for *without rainfall* respectively. Circles and error bars represent the median and 90% range of L_{Aeq} and rainfall rate for *with rainfall*, respectively.

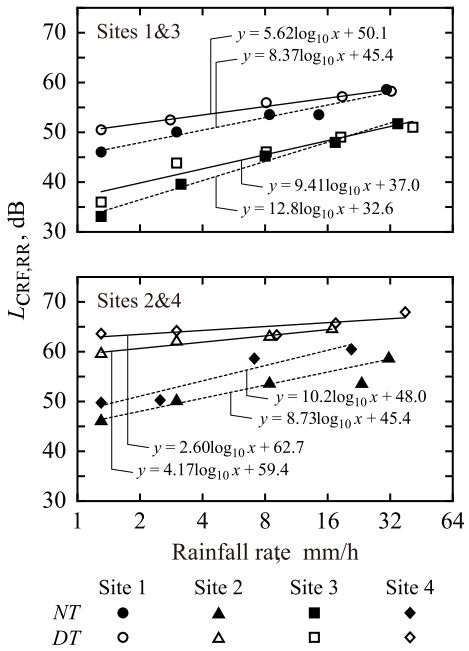

Figure 9: Relationship between rainfall rate and L_{Aeq} of the sounds caused by rainfall ($L_{CRF}(RR)$). Solid and dashed lines represent regression lines for each condition. Different symbols represent different pairs of site and time period.

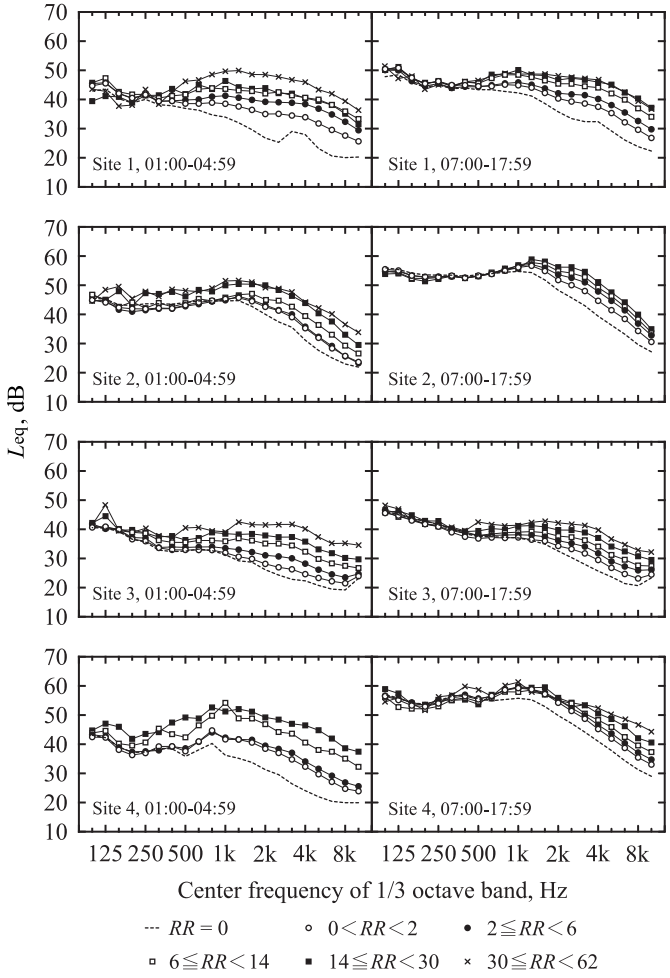

Figure 10: 1/3 Octave band spectrum of the median of L_{eq} with rainfall for each site and time period. Dashed lines represent L_{eq} for *without rainfall* as a reference. Different symbols represent different rainfall rate (*RR*) classifications.

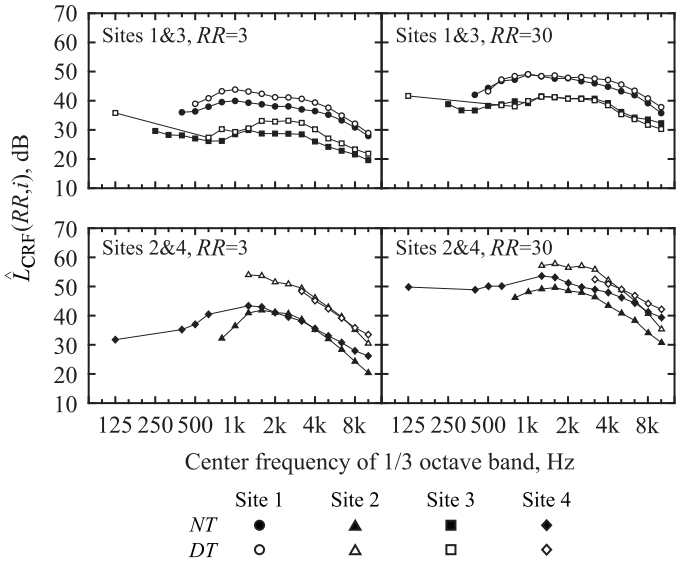

Figure 11: Estimated L_{eq} of the sounds caused by rainfall for each 1/3 octave band. Left and right panels show results for rainfall rates (*RR*s) of 3 and 30 mm/h, respectively. Different symbols represent different pairs of site and time period.

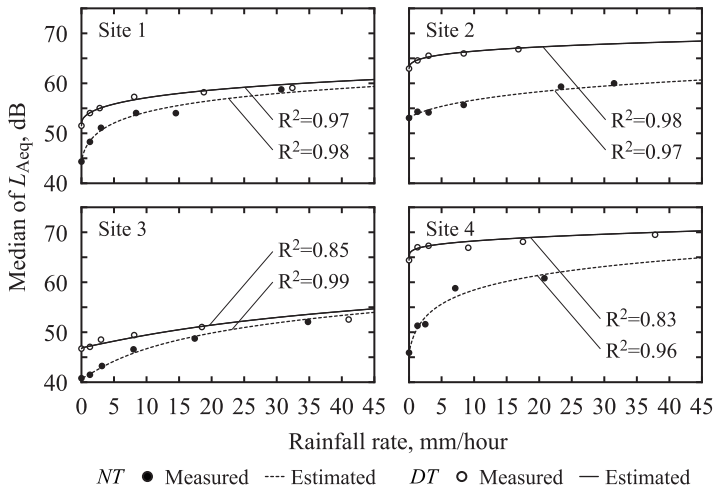

Figure 12: Measured and estimated medians of L_{Aeq} for each pair of site and time period. The estimated values were obtained from the macroscopic model defined by Eq. 3.

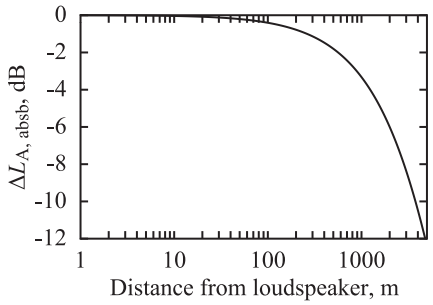

Figure 13: Attenuation of A-weighted level of speech by atmospheric absorption as a function of distance from loudspeaker ($\Delta L_{A,absb}$), where temperature is 15°C and relative humidity is 90%.

List of Tables

1 Summary of the measurement sites. 42

2 Number of samples and measurement periods for each site. Data were sampled every minute. The columns of '> 0 mm/h' and '> 40 mm/h' indicate the number of samples with rainfall and that with heavy rainfall, respectively. 43

3 Classification of rainfall rate in the present study and number of samples for each site and time period. *NT* and *DT* are time periods of 01:00–04:59 and 07:00–17:59, respectively. 44

4 Representative values of weather parameters for each classification of rainfall rate. The classification of zero means *without rainfall*. The values for rainfall rate, temperature, and relative humidity are medians, and that for wind speed is average. 45

5 L_{Aeq} estimated from the macroscopic model under the no rain and heavy rain conditions. 46

6 Maximum distance from loudspeaker to maintain the speech-to-noise ratio of +6 dB under the no rain and heavy rain conditions. 47

Table 1: Summary of the measurement sites.

Site	Installation location	Surroundings
1	Rooftop (2 levels)	On campus, many trees, quiet with few pedestrians
2	Rooftop (3 levels)	Beside major road with microphone installed some distance from road
3	1.5 m above ground	Vacant lot covered with gravel, periodic aircraft noise
4	Sidewall on 2nd floor	Beside major road with microphone installed close to road

Table 2: Number of samples and measurement periods for each site. Data were sampled every minute. The columns of '> 0 mm/h' and '> 40 mm/h' indicate the number of samples with rainfall and that with heavy rainfall, respectively.

Site	Measurement period	Number of samples		
		Total	> 0 mm/h	> 40 mm/h
1	Oct. 2, 2015–Nov. 30, 2015	66,808	2,358	13
2	Oct. 13, 2015–Nov. 30, 2015	63,068	2,681	17
3	Oct. 21, 2015–Nov. 24, 2015	41,001	2,418	25
4	Oct. 14, 2015–Nov. 30, 2015	61,627	2,551	10

Table 3: Classification of rainfall rate in the present study and number of samples for each site and time period. *NT* and *DT* are time periods of 01:00–04:59 and 07:00–17:59, respectively.

Classification	Rainfall rate	Site 1		Site 2		Site 3		Site 4	
	(RR), mm/h	*NT*	*DT*	*NT*	*DT*	*NT*	*DT*	*NT*	*DT*
1	$0 < RR < 2$	222	400	205	521	71	422	166	599
2	$2 \leqq RR < 6$	211	369	148	494	42	553	144	486
3	$6 \leqq RR < 14$	20	79	23	108	16	167	10	79
4	$14 \leqq RR < 30$	5	15	4	28	8	31	5	17
5	$30 \leqq RR < 62$	3	6	4	0	1	6	0	3

Table 4: Representative values of weather parameters for each classification of rainfall rate. The classification of zero means *without rainfall*. The values for rainfall rate, temperature, and relative humidity are medians, and that for wind speed is average.

Parameter	Classification	Site 1		Site 2		Site 3		Site 4	
		NT	*DT*	*NT*	*DT*	*NT*	*DT*	*NT*	*DT*
Rainfall rate, mm/h	0	0.0	0.0	0.0	0.0	0.0	0.0	0.0	0.0
	1	1.3	1.3	1.3	1.3	1.3	1.3	1.3	1.3
	2	3.0	2.8	3.0	3.0	3.0	3.0	2.5	3.0
	3	8.4	8.1	8.4	8.4	8.0	8.1	7.1	9.1
	4	14.5	18.8	23.4	16.8	17.4	18.7	20.8	17.5
	5	30.7	32.4	31.5	-	34.8	41.1	-	37.8
Temperature, °C	0	15.9	18.5	13.4	17.8	14.3	17.8	13.2	17.7
	1	17.2	17.4	17.2	17.1	16.4	16.9	16.9	16.8
	2	17.2	17.6	17.4	17.1	16.9	17.1	16.9	16.8
	3	17.2	18.2	17.2	17.2	12.4	17.1	17.6	16.8
	4	18.6	18.2	17.8	16.9	17.9	17.1	17.6	16.7
	5	19.2	18.0	17.8	-	17.9	17.2	-	16.7
Relative humidity, %	0	77.0	67.0	83.0	66.0	81.0	65.0	83.0	66.0
	1	89.0	92.5	93.0	94.0	95.0	92.0	93.0	94.0
	2	88.0	93.0	91.0	95.0	95.0	92.0	90.0	94.0
	3	88.0	93.0	96.0	95.0	89.0	92.0	97.0	94.0
	4	95.0	93.0	97.0	94.5	95.0	92.0	97.0	94.0
	5	94.0	93.5	97.0	-	95.0	92.0	-	94.0
Wind speed, m/s	0	0.7	0.9	1.3	1.7	0.8	1.4	0.5	1.1
	1	1.1	0.9	0.9	1.2	0.6	0.5	0.6	0.7
	2	1.1	0.8	0.8	1.2	0.7	0.5	0.5	0.7
	3	1.7	0.8	0.7	1.8	1.1	0.8	0.0	1.5
	4	0.5	1.0	0.5	2.3	0.6	0.8	0.0	1.2
	5	0.4	0.8	0.3	-	0.0	1.7	-	1.3

Table 5: L_{Aeq} estimated from the macroscopic model under the no rain and heavy rain conditions.

Rainfall rate,	Site 1		Site 2		Site 3		Site 4	
mm/h	*NT*	*DT*	*NT*	*DT*	*NT*	*DT*	*NT*	*DT*
0	44.3	51.5	53.1	62.9	40.8	46.7	45.9	64.4
40	59.0	60.4	60.3	68.3	53.4	54.2	64.4	70.1
80	61.4	62.4	62.5	69.4	57.1	57.4	67.4	71.4
160	63.9	64.6	64.9	70.7	60.9	61.0	70.5	73.2
								[dB]

Table 6: Maximum distance from loudspeaker to maintain the speech-to-noise ratio of +6 dB under the no rain and heavy rain conditions.

Rainfall rate,	Site 1		Site 2		Site 3		Site 4	
mm/h	*NT*	*DT*	*NT*	*DT*	*NT*	*DT*	*NT*	*DT*
0	1,385	854	759	335	1,704	1,189	1,252	292
40	473	419	423	201	742	698	292	168
80	384	351	348	180	554	541	219	147
160	306	286	279	158	401	398	161	122
								[m]